A&A 541, A143 (2012)
DOI: 10.1051/0004-6361/201218773

Astronomy & Astrophysics

NLTE determination of the calcium abundance and 3D corrections in extremely metal-poor stars⋆,⋆⋆

M. Spite[1], S. M. Andrievsky[1,2], F. Spite[1], E. Caffau[3,1], S. A. Korotin[2], P. Bonifacio[1], H.-G. Ludwig[3], P. François[1], and R. Cayrel[1]

[1] GEPI Observatoire de Paris, CNRS, Université Paris Diderot, 92195 Meudon Cedex, France
e-mail: monique.spite@obspm.fr
[2] Department of Astronomy and Astronomical Observatory, Odessa National University, T.G. Shevchenko Park, 65014, Odessa; and Isaac Newton Institute of Chile, Odessa Branch, Ukraine
[3] Zentrum für Astronomie der Universität Heidelberg, Landessternwarte, Königstuhl 12, 69117 Heidelberg, Germany

Received 4 January 2012 / Accepted 19 March 2012

ABSTRACT

Context. Calcium is a key element for constraining the models of chemical enrichment of the Galaxy.
Aims. Extremely metal-poor stars contain the fossil records of the chemical composition of the early Galaxy and it is important to compare Ca abundance with abundances of other light elements, that are supposed to be synthesized in the same stellar evolution phases.
Methods. The NLTE profiles of the calcium lines were computed in a sample of 53 extremely metal-poor stars with a modified version of the program MULTI, which allows a very good description of the radiation field.
Results. With our new model atom we are able to reconcile the abundance of Ca deduced from the Ca I and Ca II lines in Procyon. This abundance is found to be solar. We find that $\overline{[Ca/Fe]} = 0.50 \pm 0.09$ in the early Galaxy, a value slightly higher than the previous LTE estimations. The scatter of the ratios [X/Ca] is generally smaller than the scatter of the ratio [X/Mg] where X is a "light metal" (O, Na, Mg, Al, S, and K) with the exception of Al. These scatters cannot be explained by error of measurements, except for oxygen. Surprisingly, the scatter of [X/Fe] is always equal to, or even smaller than, the scatter around the mean value of [X/Ca]. We note that at low metallicity, the wavelength of the Ca I resonance line is shifted relative to the (weaker) subordinate lines, a signature of the effect of convection. The Ca abundance deduced from the Ca I resonance line (422.7 nm) is found to be systematically smaller at very low metallicity than the abundance deduced from the subordinate lines. Our computations of the effects of convection (3D effects) are not able to explain this difference. A fully consistent 3D NLTE model atmosphere and line formation scheme would be necessary to fully capture the physics of the stellar atmosphere.

Key words. line: formation – line: profiles – stars: abundances – supernovae: general – Galaxy: evolution

1. Introduction

An homogeneous sample of 53 metal-poor stars, most of them extremely metal-poor (EMP stars with [Fe/H] < −2.9), has been observed by Cayrel et al. (2004), and Bonifacio et al. (2007, 2009). The aim of this paper is to determine the calcium abundance in these stars more precisely. These low mass stars have been formed at the very early phases of the Galaxy and the chemical composition of their atmosphere reflects the yields of the first massive type II supernovae which have a very short life-time. These supernovae produce more "α-elements" (O, Mg, Si, S, Ca) than "iron-peak" elements. In contrast, less massive type I supernovae, which have a much longer life-time and explode later, produce more iron-peak elements than α-elements. As a consequence in the atmosphere of the EMP stars formed at the beginning of the Galaxy a relative enhancement of the α-elements (compared to the Sun) is observed. The level of this overabundance is one of the fundamental parameters of the chemical evolution models of the Galaxy.

On the other hand, the relative production of the α-elements in a supernova depends on the mass of this supernova (e.g. Kobayashi et al. 2006): [Ca/Fe] tends to be lower for more massive supernovae. Therefore the level of [Ca/Fe] in the early Galaxy constrains the IMF in the early times.

Moreover, Cayrel et al. (2004) and Bonifacio et al. (2009) have shown that for [Fe/H] < −2.7 the abundances of the α-elements relative to iron ([Mg/Fe], [Si/Fe], [Ca/Fe], and [Ti/Fe]) are constant with a small scatter but that surprisingly the scatters of these elements relative to magnesium (another α-element) are larger. This larger scatter cannot be explained by a lower precision of the abundance of magnesium. Cayrel et al. (2004) and Bonifacio et al. (2009) computed the abundances under the LTE hypothesis. The non-LTE (NLTE) abundances of two α-elements Mg and S have been then computed in Andrievsky et al. (2010) and Spite et al. (2011). These papers confirm that the scatter of abundance ratios is generally larger when Mg replaces Fe as a reference element. It is then interesting

⋆ Based on observations obtained with the ESO Very Large Telescope at Paranal Observatory, Chile (Large Programme "First Stars", ID 165.N-0276(A); P.I.: R. Cayrel).
⋆⋆ The NLTE corrections of the Ca lines are available in electronic form at the CDS via anonymous ftp to
cdsarc.u-strasbg.fr (130.79.128.5) or via
http://cdsarc.u-strasbg.fr/viz-bin/qcat?J/A+A/541/A143

to check wether the link between the abundance of Ca and the abundance of the other α-elements is closer.

In this paper we have carried out a NLTE analysis of the calcium abundance in the atmosphere of these EMP stars and have tried to estimate the influence of convection (3D computations).

For this new analysis we have used the resonance line of Ca I and about 15 subordinate lines. We have also used the line of the Ca II infrared triplet at 866.21 nm. Unfortunately, the two other lines of this triplet (at 849.81 and 854.21 nm) are outside the observed spectral range.

2. Star sample and model parameters

The spectra of the stars investigated here have been presented in detail in Cayrel et al. (2004) and Bonifacio et al. (2007). The observations were performed with the high-resolution spectrograph UVES at ESO-VLT (Dekker et al. 2000). The resolving power of the spectrograph is $R \approx 45\,000$, with about five pixels per resolution element and the signal-to-noise ratio per pixel is typically about 150.

The fundamental parameters of the models (effective temperature $T_{\rm eff}$, logarithm of the gravity $\log g$, and metallicity) have been derived by Cayrel et al. (2004) for the giants and Bonifacio et al. (2007) for the turnoff stars. Briefly, temperatures of the giants are deduced from the colors with the calibration of Alonso et al. (1999, 2001), and temperatures of the turnoff stars from the wings of the Hα line. Moreover we checked that these Hα temperatures agreed with the temperatures derived from the color $V - K$ and the calibration of Alonso et al. (1996). The gravities are derived from the ionization equilibrium of iron (under the LTE approximation) and we note that they might be affected by NLTE effects. The parameters of the models are repeated in Table 1 for the reader's convenience.

3. Determination of the calcium abundance

The NLTE profiles of the calcium lines were computed with a modified version of the code MULTI (Carlsson 1986; Korotin et al. 1999), which allows a very good description of the radiation field. This version includes opacities from ATLAS9 (Kurucz 1992), which modify the intensity distribution in the UV.

3.1. Atmospheric models

For these computations we used Kurucz models without overshooting (Castelli et al. 1997). These models have been shown to provide LTE abundances very similar (within 0.05 dex) to those of the MARCS models used by Cayrel et al. (2004) and Bonifacio et al. (2009). The solar model was taken from Castelli[1] with a chromospheric contribution from the VAL-3C model of Vernazza et al. (1981) and the corresponding microturbulence distribution.

3.2. Atomic model

Our model atom of calcium is similar to the one used by Mashonkina et al. (2007) but it includes some more levels and more recent atomic data. Seventy levels of Ca I, thirty-eight levels of Ca II, and the ground state of Ca III were taken into account; in addition, more than 300 levels of Ca I and Ca II were included to keep the condition of the particle number conservation in LTE. The fine structure was taken into account for the levels $3d^2D$ and $4p^2P^0$ of Ca II.

The energy levels were taken from the NIST atomic spectra database (Sugar & Corliss 1985). The ionization cross-sections were taken from TOPBASE. The oscillator strengths of the Ca I and Ca II lines were taken from the most recent estimations: Wiese et al. (1969), Smith & Raggett (1981), Smith (1988), Theodosiou (1989), Morton (1991), Kurucz (1993), and from TOPBASE for the lines occuring between non-splitted levels. For the forbidden transitions, we used TOPBASE and Hirata & Horaguchi (1995).

We considered 351 transitions in detail; for 375 weak transitions the radiative rates were fixed. Collisional rates between the ground level and the ten lower levels of Ca I were taken from Samson & Berrington (2001). For Ca II, collisional rates were taken from Meléndez et al. (2007) instead of those of Burgess et al. (1995) used by Mashonkina et al. (2007) for the lower seven terms.

For the other transitions (without data) we used for allowed transitions, the Van Regemorter (1962) formula, and for the forbidden transitions the Allen (1973) formula.

Electron impact ionization cross-sections were calculated by applying the formula of Seaton (1962), with threshold photoionization cross-sections from the Opacity-Project data.

Collisions with hydrogen atoms were computed using the Steenbock & Holweger (1984) formula. The cross sections calculated with this formula were multiplied by a scaling factor $S_{\rm H}$: the "efficiency" of the hydrogenic collisions. This factor was constrained empirically by comparing the Ca abundance obtained from different lines in the Sun and in some reference stars (Procyon, HD 140283, HD 122563). The best agreement was obtained with $S_{\rm H} = 0.1$ which agrees well with Ivanova et al. (2002) and Mashonkina et al. (2007).

3.3. Consistency check

To test the Ca atom model, we computed the profiles of the calcium lines in the Sun, in Procyon, and in two classical metal-poor stars HD 122563, and HD 140283. The synthetic spectra were computed following the procedure described in Korotin (2008): we calculated the departure coefficients factors "b" for the Ca lines with MULTI and then used these factors in the LTE synthetic spectrum code.

- For the Sun we used the solar atmosphere model computed by Castelli with a chromospheric contribution following Vernazza et al. (1981, see Sect. 3.1). A micro turbulence velocity $\xi_{\rm t} = 1.0$ km s^{-1} was adopted in the atmosphere.
  We computed the profile of 49 lines of Ca I and 17 lines of Ca II. The $\log gf$ value of the lines and the broadening parameter due to collisions with hydrogen atoms, $\log \gamma_{VW}/N_{\rm H}$ (for $T = 10\,000$ K), are given in Table 2. We found $\log \epsilon({\rm Ca}) = 6.31 \pm 0.05$ from the Ca I lines and $\log \epsilon({\rm Ca}) = 6.30 \pm 0.07$ from the Ca II lines. These values agree well with the meteoritic calcium abundance $\log \epsilon({\rm Ca}) = 6.31 \pm 0.02$ (Lodders et al. 2009) and the photospheric abundances derived by Asplund et al. (2009) for the solar atmosphere: $\log \epsilon({\rm Ca}) = 6.34 \pm 0.04$ (a value that includes 3D effects).
  For most of the lines in Table 2, the broadening parameter $\log \gamma_{VW}/N_{\rm H}$ (for $T = 10\,000$ K) due to collisions with hydrogen atoms, was taken from the precise calculations of Anstee & O'Mara (1995), Barklem & O'Mara (1997, 1998), and Barklem et al. (1998). For the other lines, this parameter

[1] http://wwwuser.oats.inaf.it/castelli/sun/ap00t5777g44377k1asp.dat

Table 1. Program stars and their parameters.

1 Star	2 $T_{\rm eff}$ K	3 log g	4 $\xi_{\rm t}$ km s^{-1}	5 [Fe/H]	6 log ϵ(Ca) sub. lines	7 N	8 σ	9 log ϵ(Ca) 422.67 nm	10 log ϵ(Ca) 866.22 nm	11 [Ca/H]	12 [Ca/Fe]
turnoff stars											
BS 16023–046	6360	4.5	1.4	–2.97	3.77	8	0.09	3.54	3.74	–2.59	0.38
BS 16968–061	6040	3.8	1.5	–3.05	3.77	11	0.08	3.70	3.70	–2.59	0.46
BS 17570–063	6240	4.8	0.5	–2.92	3.80	12	0.06	3.70	3.70	–2.56	0.36
CS 22177–009	6260	4.5	1.2	–3.10	3.64	11	0.09	3.52	3.61	–2.72	0.38
CS 22888–031	6150	5.0	0.5	–3.28	3.45	10	0.11	3.33	3.36	–2.91	0.37
CS 22948–093	6360	4.3	1.2	–3.43	3.49	4	0.06	3.37	3.59	–2.87	0.56
CS 22953–037	6360	4.3	1.4	–2.89	3.83	11	0.10	3.71	3.73	–2.53	0.36
CS 22965–054	6090	3.8	1.4	–3.04	3.93	12	0.22	3.78	3.71	–2.43	0.61
CS 22966–011	6200	4.8	1.1	–3.07	3.69	11	0.10	3.60	3.51	–2.67	0.40
CS 29499–060	6320	4.0	1.5	–2.70	4.05	14	0.12	3.94	4.08	–2.31	0.39
CS 29506–007	6270	4.0	1.7	–2.91	4.05	14	0.09	3.95	3.85	–2.31	0.60
CS 29506–090	6300	4.3	1.4	–2.83	4.09	14	0.11	3.90	3.93	–2.27	0.56
CS 29518–020	6240	4.5	1.7	–2.77	4.03	10	0.18	–	–	–2.33	0.44
CS 29518–043	6430	4.3	1.3	–3.24	3.71	11	0.17	3.54	3.60	–2.65	0.59
CS 29527–015	6240	4.0	1.6	–3.55	3.35	4	0.20	3.06	3.26	–3.01	0.54
CS 30301–024	6330	4.0	1.6	–2.75	4.16	15	0.08	4.00	4.04	–2.20	0.55
CS 30339–069	6240	4.0	1.3	–3.08	3.81	11	0.13	3.79	3.77	–2.55	0.53
CS 31061–032	6410	4.3	1.4	–2.58	4.23	14	0.14	4.16	–	–2.13	0.45
giants											
HD 2796	4950	1.5	2.1	–2.47	4.33	16	0.09	4.32	4.45	–2.03	0.43
HD 122563	4600	1.1	2.0	–2.82	3.97	16	0.08	3.93	3.95	–2.39	0.42
HD 186478	4700	1.3	2.0	–2.59	4.31	16	0.11	4.33	4.12	–2.05	0.53
BD +17°3248	5250	1.4	1.5	–2.07	4.74	14	0.05	4.74	4.70	–1.62	0.45
BD –18°5550	4750	1.4	1.8	–3.06	3.88	16	0.09	3.72	3.80	–2.48	0.58
CD –38°245	4800	1.5	2.2	–4.19	2.72	4	0.13	2.30	2.64	–3.64	0.55
BS 16467–062	5200	2.5	1.6	–3.77	3.22	9	0.23	2.97	2.97	–3.14	0.63
BS 16477–003	4900	1.7	1.8	–3.36	3.59	16	0.12	3.32	3.45	–2.77	0.59
BS 17569–049	4700	1.2	1.9	–2.88	4.04	16	0.14	4.06	3.90	–2.32	0.56
CS 22169–035	4700	1.2	2.2	–3.04	3.64	16	0.09	3.34	3.70	–2.72	0.32
CS 22172–002	4800	1.3	2.2	–3.86	3.11	11	0.09	2.52	3.11	–3.25	0.61
CS 22186–025	4900	1.5	2.0	–3.00	3.89	15	0.08	3.73	3.90	–2.47	0.53
CS 22189–009	4900	1.7	1.9	–3.49	3.27	12	0.07	2.95	3.40	–3.09	0.40
CS 22873–055	4550	0.7	2.2	–2.99	3.89	16	0.09	3.73	3.75	–2.47	0.52
CS 22873–166	4550	0.9	2.1	–2.97	3.92	16	0.09	3.84	3.92	–2.44	0.53
CS 22878–101	4800	1.3	2.0	–3.25	3.68	16	0.12	3.30	3.65	–2.68	0.57
CS 22885–096	5050	2.6	1.8	–3.78	3.10	8	0.11	2.83	2.98	–3.26	0.52
CS 22891–209	4700	1.0	2.1	–3.29	3.58	16	0.08	3.33	3.45	–2.78	0.51
CS 22892–052*	4850	1.6	1.9	–3.03	3.84	14	0.12	3.65	3.80	–2.52	0.51
CS 22896–154	5250	2.7	1.2	–2.69	4.12	16	0.12	4.01	4.00	–2.23	0.46
CS 22897–008	4900	1.7	2.0	–3.41	3.45	11	0.12	3.05	3.35	–2.91	0.50
CS 22948–066	5100	1.8	2.0	–3.14	3.69	14	0.09	3.45	3.60	–2.67	0.47
CS 22949–037*	4900	1.5	1.8	–3.97	3.01	9	0.10	2.75	3.20	–3.35	0.61
CS 22952–015	4800	1.3	2.1	–3.43	3.29	12	0.08	2.95	3.25	–3.07	0.36
CS 22953–003	5100	2.3	1.7	–2.84	3.89	16	0.10	3.74	3.85	–2.47	0.37
CS 22956–050	4900	1.7	1.8	–3.33	3.69	16	0.09	3.49	3.75	–2.67	0.66
CS 22966–057	5300	2.2	1.4	–2.62	4.23	16	0.09	4.21	4.10	–2.13	0.49
CS 22968–014	4850	1.7	1.9	–3.56	3.06	10	0.10	2.67	2.89	–3.29	0.27
CS 29491–053	4700	1.3	2.0	–3.04	3.89	16	0.08	3.68	3.85	–2.47	0.57
CS 29495–041	4800	1.5	1.8	–2.82	4.05	16	0.07	4.00	3.95	–2.31	0.51
CS 29502–042	5100	2.5	1.5	–3.19	3.55	13	0.08	3.41	3.40	–2.81	0.38
CS 29516–024	4650	1.2	1.7	–3.06	3.99	16	0.12	3.93	–	–2.37	0.69
CS 29518–051	5200	2.6	1.4	–2.69	4.14	16	0.07	4.07	4.10	–2.22	0.47
CS 30325–094	4950	2.0	1.5	–3.30	3.61	15	0.08	3.51	3.55	–2.75	0.55
CS 31082–001	4825	1.5	1.8	–2.91	4.01	14	0.08	4.01	3.90	–2.35	0.56

Notes. The stars marked with an asterisk are carbon-rich. Columns 2 to 5 give the main parameters of the stars. Column 6 is the NLTE calcium abundance deduced from the subordinate Ca I lines with the number of lines and the standard deviation (Cols. 7 and 8). Columns 9 and 10 list the abundance of Ca derived from a NLTE computation of the 422.67 and 866.22 nm lines. The last two columns give [Ca/H] and [Ca/Fe] based on the calcium abundance deduced from the Ca I subordinate lines.

Table 2. Parameters of the Ca lines used in the solar spectrum. $\gamma_1 = \log \gamma_{VW}/N_H$ for a temperature of 10 000 K.

Line (nm)	log gf	Ref.	γ_1	Ref.	Line (nm)	log gf	Ref.	γ_1	Ref.
Ca I					Ca I				
410.8526	–0.824	1	–6.97	11	616.6439	–1.143	4	–7.15	9
422.6728	0.244	6	–7.56	9	616.9042	–0.797	4	–7.15	9
428.3011	–0.220	3	–7.50	12	616.9563	–0.478	4	–7.15	9
428.9367	–0.300	3	–7.50	12	643.9075	0.390	4	–7.57	9
430.2528	0.280	3	–7.50	12	645.5598	–1.340	2	–7.65	1
431.8652	–0.211	3	–7.50	12	646.2567	0.262	4	–7.57	9
435.5079	–0.420	3	–6.80	11	647.1662	–0.686	4	–7.57	9
442.5437	–0.360	3	–7.16	9	649.3781	–0.109	4	–7.57	9
443.4957	–0.010	3	–7.16	9	649.9650	–0.818	4	–7.57	9
443.5679	–0.523	3	–7.16	9	657.2779	–4.296	6	–7.69	9
445.4779	0.260	3	–7.16	9	671.7681	–0.523	4	–7.14	9
445.6616	–1.660	3	–7.16	9	714.8150	0.137	4	–7.80	1
451.2268	–1.892	4	–7.26	1	720.2200	–0.262	7	–7.80	1
452.6928	–0.548	4	–7.00	11	732.6145	–0.208	7	–7.30	11
457.8551	–0.697	4	–7.00	11	1034.3820	–0.409	5	–7.12	9
468.5268	–0.880	3	–6.40	11					
518.8844	–0.115	4	–7.00	11	Ca II				
526.0387	–1.719	4	**–7.51**	**9**	393.3663	0.104	6	–7.76	9
526.1704	–0.579	4	**–7.51**	**9**	396.8469	–0.201	6	–7.76	9
526.5556	–0.114	4	**–7.51**	**9**	500.1479	–0.506	10	–7.34	1
534.9465	–0.310	4	–7.44	12	645.6875	0.412	10	–6.61	11
551.2980	–0.464	7	–7.00	11	820.1722	0.300	2	–7.00	11
558.1965	–0.555	4	–7.54	9	824.8796	0.570	2	–7.00	11
558.8749	0.358	4	–7.54	9	825.4730	–0.400	2	–7.00	11
559.0114	–0.571	4	–7.54	9	849.8023	–1.416	8	–7.68	9
559.4462	0.097	4	–7.54	9	854.2091	–0.463	8	–7.68	9
585.7451	0.240	4	–7.12	11	866.2141	–0.723	8	–7.68	9
586.7562	–1.570	7	–7.00	11	891.2068	0.631	10	–7.21	11
610.2723	–0.770	4	–7.19	9	892.7356	0.808	10	–7.21	11
612.2217	–0.319	4	–7.19	9	985.4759	–0.228	10	–7.00	11
615.6023	–2.497	5	–7.15	9	989.0628	1.270	10	–7.01	11
616.1297	–1.268	4	–7.15	9	993.1374	0.051	2	–7.00	11
616.2173	–0.090	3	–7.19	9	1183.8997	0.290	2	–7.36	11
616.3755	–1.286	7	–7.15	9	1194.9745	–0.010	2	–7.36	11

References. 1: VALD; 2: Wiese et al. (1969); 3: Wiese & Martin (1980); 4: Smith & Raggett (1981); 5: Kurucz & Bell (1995); 6: Morton (1991); 7: Smith et al. (1988); 8: Theodosiou (1989); 9: Anstee & O'Mara (1995); Barklem & O'Mara (1997, 1998); 10: opacity project; 11: fit of the Solar atlas; 12: Unsöld formula + fit of the Solar atlas.

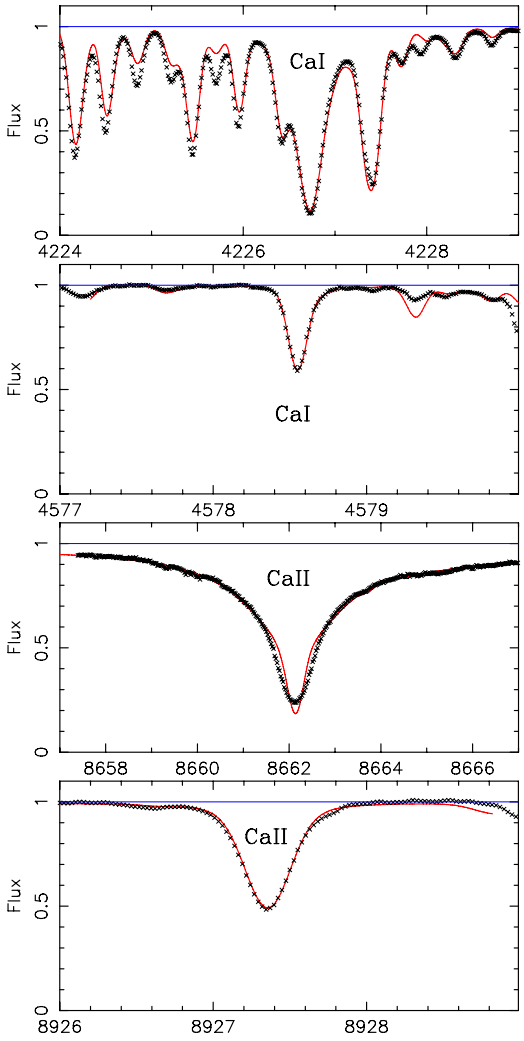

Fig. 1. Profiles of Ca I and Ca II lines in Procyon. The wavelengths are in Å. The small crosses represent the observed spectrum and the (red) line the computed profile. With our model atom, the observed and computed profiles of the Ca I and Ca II lines agree well.

was derived from the fit of the solar atlas (Kurucz et al. 1984). These values are, for the high excitation lines of Ca II, higher than the values obtained from the Unsöld or Kurucz approximation. However, they agree well with the values obtained by Ivanova et al. (2002), who note that the use of the Unsöld or Kurucz approximation often leads to an underestimation of the broadening parameter.

- We retrieved the spectrum of Procyon from the UVES POP (Bagnulo et al. 2003). Procyon has a solar-like chemical composition, and its surface gravity, derived from Hipparcos measurements (Perryman et al. 1997), is log g = 3.96. We adopted a microturbulence ξ_t = 1.8 km s^{-1}. For this star, Mashonkina et al. (2007) adopting $T_{\rm eff}$ = 6510 K (Mashonkina et al. 2003) or $T_{\rm eff}$ = 6590 K (Korn et al. 2003) found a subsolar abundance of Ca and a difference of about 0.2 dex between the NLTE calcium abundance derived from the Ca I and Ca II lines.
  With $T_{\rm eff}$ = 6510 K and our model atom, we derive for Procyon a near solar calcium abundance and a much better agreement between Ca I and Ca II: log ϵ(Ca) = 6.25±0.04 from Ca I lines and 6.27 ± 0.06 from Ca II lines (Fig. 1).
- We also tested our model on two classical metal-poor stars: HD 122563 (a star from our sample of giants) and HD 140283. The spectrum of HD 140283 was retrieved from the ESO POP (Bagnulo et al. 2003). For HD 122563 we adopted the parameters given in Table 1, and for HD 140283 the parameters given by Hosford et al. (2009): $T_{\rm eff}$ = 5750 K, log g = 3.4, ξ_t = 1.5 km s^{-1}. The agreement is good. From the Ca I lines we obtain log ϵ(Ca) = 4.12 ± 0.04 and from the Ca II lines log ϵ(Ca) = 4.08 ± 0.05. In Fig. 2 we show the fit between the observed spectrum of HD 140283 and the synthetic profiles computed with log ϵ(Ca) = 4.12.

4. Calcium abundance in the EMP stars sample

4.1. Comparison between the different systems

In Fig. 3 we show the influence of the NLTE effects on the profile of some typical calcium lines measurable in extremely metal-poor stars. Evidently, in particular the wings of the lines of the

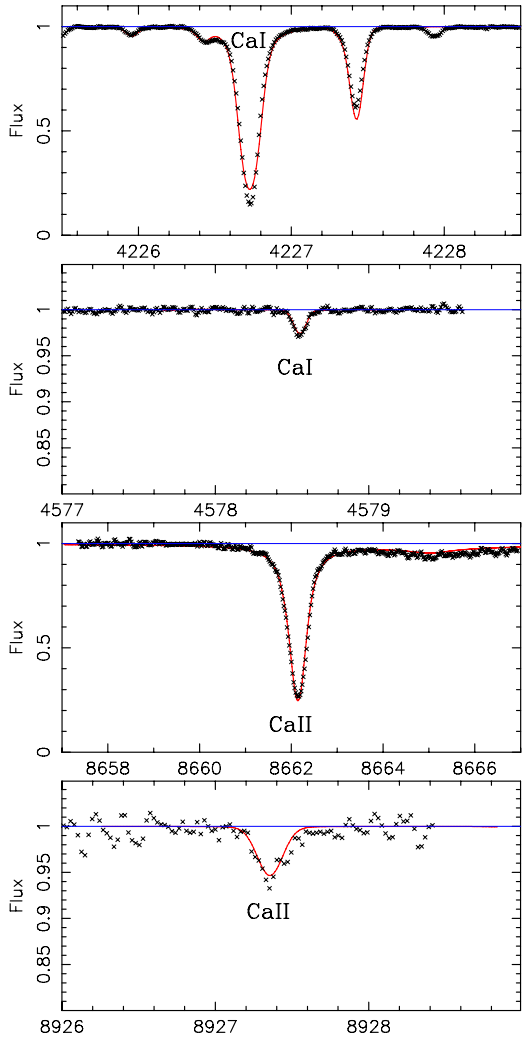

Fig. 2. Profiles of Ca I and Ca II lines in HD 140283. The wavelengths are in Å. The symbols are the same as in Fig. 1. The observed spectrum and the synthetic profiles computed with log ϵ(Ca) = 4.12 agree well.

Ca II infrared triplet are not sensitive to NLTE effects until the wings are strong enough.

In Fig. 4 the correction NLTE-LTE is given as a funtion of the temperature, the gravity, and the calcium abundance for the Ca I resonance line and a typical subordinate line of Ca I. The NLTE corrections for different temperatures, gravities, and abundances for all the Ca lines used in this analysis (Table 2) are available in electronic form[2]. The influence of the complex NLTE effects as a function of the stellar parameters and of the characteristics of the lines has been discussed by Mashonkina et al. (2007) and Merle et al. (2011).

In Table 1 we give for each star the mean abundance derived from the subordinate lines of Ca I (Col. 6), the number of lines used for the analysis (Col. 7), and the internal error (Col. 8). Column 9 lists the abundance deduced from the resonance line of Ca I, and Col. 10 the abundance computed from the infra-red Ca II line at 866.21 nm (only this line of the red Ca II triplet is in the wavelength range of our spectra). Columns 11 and 12 list [Ca/H] and [Ca/Fe] deduced from the subordinate lines of Ca I. For an easier comparison to the previous "First Stars" papers, the solar abundance of calcium was taken from Grevesse & Sauval (2000) as in Cayrel et al. (2004): $\log\epsilon_{(\mathrm{Ca})\odot} = 6.36$.

[2] http://cdsarc.u-strasbg.fr/viz-bin/qcat?J/A+A/541/A143

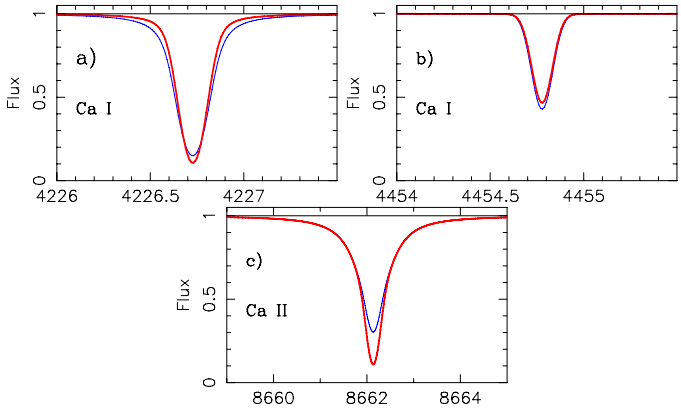

Fig. 3. Profiles of three Ca lines computed for a giant star with [Ca/H] ≈ −2.5 with LTE (thin blue line) and NLTE (thick red line) hypotheses. The wavelengths are given in Å. **a)** The NLTE profile of the Ca I resonance line is narrower in the wings and deeper in the core. **b)** In a Ca I subordinate line, for the same abundance of calcium the equivalent width computed under the NLTE hypothesis is slightly smaller. **c)** The NLTE correction is important for the strong IR Ca II line (note that the scale in wavelength is different for this line), but the wings are not affected and a reliable calcium abundance can be deduced from these wings via LTE analysis.

The oscillator strengths of the calcium lines measured in our metal-poor stars were updated (to be the same as in Sect. 3.2). As a consequence, for some lines (Table 2) they are slightly different from the log gf values used in Cayrel et al. (2004) and Bonifacio et al. (2009).

The abundance of Ca was deduced from the equivalent widths for the subordinate lines of Ca I. But for the resonance line, which is often strong and slightly blended with Fe I and CH lines, a fit of the profile was made. The Ca abundance was generally deduced from a fit of the wings (insensitive to NLTE effects) for the red Ca II lines. However, in the turnoff stars and in the most metal-poor giants, the wings almost disappear (when the equivalent widths are less than 400 mÅ) and in this case, equivalent widths were used.

In Fig. 5 we compare the abundances of calcium derived from these different systems. The abundance deduced from the line of the infrared triplet of Ca II at 862.21 nm is, as a mean, 0.07 dex lower than the abundance deduced from the subordinate lines of Ca I (Fig. 5a). This small difference is quite satisfactory since the abundance deduced from the Ca II lines depends on the surface gravity of the model, and this gravity can be affected by a systematic error since it has been derived from the ionization equilibrium of iron under the LTE hypothesis (see Cayrel et al. 2004).

In Fig. 5b, the calcium abundance derived from the subordinate lines of Ca I is compared to the abundance deduced from the Ca I resonance line at 422.67 nm. It is well known that in very metal-poor stars, under the LTE hypothesis, this resonance line leads to an underestimation of the calcium abundance: e.g. Magain (1988), Ryan et al. (1996). But it was expected that NLTE computations of the lines would remove this effect. For one typical metal-poor giant CS 22172-02 we show in Fig. 6 the observed spectrum and theoretical spectra computed with abundances log ϵ(Ca) = 2.52 (best fit), 2.8 and 3.1. The subordinate lines lead to a Ca abundance of 3.11; this value is well established: seven of the subordinate lines have an equivalent width stronger than 9 mÅ and the scatter in abundance is only 0.09 dex.

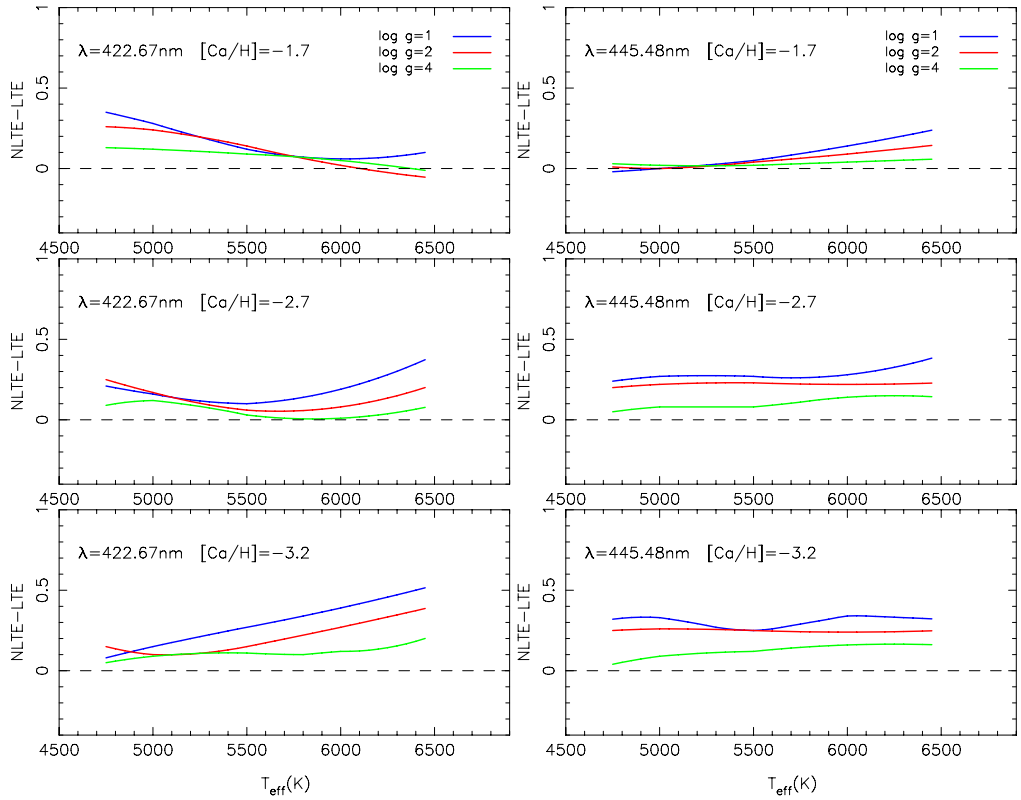

Fig. 4. NLTE corrections for the Ca I resonance line at 422.67 nm and for a typical subordinate line of Ca I at 445.48 nm.

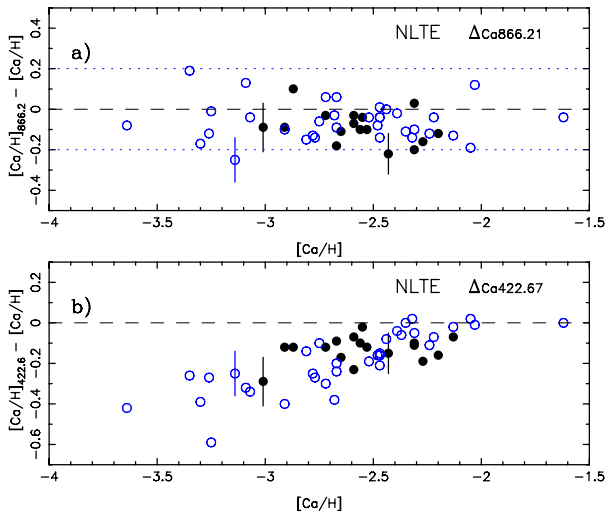

Fig. 5. Difference between [Ca/H] deduced from the subordinate lines of Ca I and [Ca/H] deduced from **a)** the infrared triplet of Ca II and **b)** the resonance line of Ca I. The filled circles represent the turnoff stars and the open symbols the giants. The error bar on [Ca/H], Δ Ca 866.21 and Δ Ca 422.67 is generally less than 0.1dex. It is indicated only when it exceeds 0.1 dex. **a)** The Ca abundance deduced from the line of the infrared triplet is, as a mean, 0.07 dex lower than the abundance derived from the subordinate lines of Ca I. **b)** For [Ca/H] ≈ −2, the abundance deduced from the Ca I resonance line agrees quite well with the abundances deduced from subordinate lines, but a discrepancy appears and increases linearly when [Ca/H] decreases. It reaches about 0.4 dex for [Ca/H]= –3.5.

A similar discrepancy has been observed, after NLTE computations, in several metal-poor stars by Mashonkina et al. (2007) and the authors suggested that the explanation could

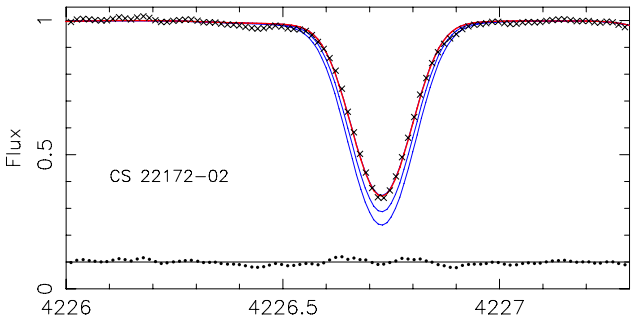

Fig. 6. Observed profile of the resonance line of Ca I (crosses) for one typical metal-poor giant compared to theoretical profiles computed with log ϵ(Ca) = 2.52 (thick red line), 2.8 and 3.1 (thin blue lines). The wavelengths are in Å. The (very small) difference between the observed spectrum and the profile computed with log ϵ(Ca) = 2.52 is shown at the bottom of the figure (dots, shifted by 0.1). For this star, the subordinate lines lead to log ϵ(Ca) = 3.11 (Table 1).

lie with the 1D atmospheric models adopted for the computations, since the Ca I resonance line is formed over a more extended range of atmospheric depths than the subordinate lines.

4.2. Influence of convection – 3D models

4.2.1. Shift of the calcium lines

The atmospheres of cool stars are not static. Velocity and intensity fluctuations caused by convection are observed in the Sun (Rutten et al. 2004) and in metal-poor stars. Ramírez et al. (2010) found that in HD 122563 (a star of our sample of giants) the cores of the Fe I lines are shifted relative to the mean radial velocity of the star, this shift increases with the equivalent width of

the line. Weaker lines form in deeper layers, where the granulation velocities and intensity contrast are higher. We also observe this phenomenon for the calcium lines in all stars of our sample. The radial velocity of the stars were determined from a constant set of iron lines, and relative to this "zero point", the radial velocity derived from the Ca I resonance line is about 0.4 km s^{-1} higher in the giants and 0.2 km s^{-1} higher in the dwarfs. In contrast, the radial velocity derived from the (weak) subordinate calcium lines is about 0.4 km s^{-1} lower in the giants and about 0.2 km s^{-1} lower in the dwarfs. (We were able to measure precisely the shift of the subordinate lines only on the "blue spectra" when these lines were larger than 20 mÅ.) At the resolution of our VLT/UVES spectra with $R \approx 45\,000$, the asymmetry of the lines cannot be reliably measured.

The shift of the Ca I resonance line does not clearly depend on [Ca/H], and therefore it does not seem that there is a clear correlation between the shift of the Ca lines and the discrepancy between the abundances deduced from the resonance or the subordinate lines.

4.2.2. Abundance correction

The largest abundance corrections caused by granulation effects occur at low metallicities. This is mainly because the difference between the 1D and 3D predictions for the mean temperature of the outer layers of metal-poor stars is very large (see e.g. González Hernández et al. 2010). We tried to investigate the change in abundances caused by thermal inhomogeneities and differences in formation depth (3D corrections hereafter) for the Ca I resonance line at 422.67 nm and for a typical subordinate line of Ca I at 445.48 nm.

- For a representative turnoff star, we used a 3D-CO5BOLD model (Freytag et al. 2002, 2011) from the CIFIST grid (see Ludwig et al. 2009) with parameters ($T_{\rm eff}$, $\log g$, [Fe/H]): 6270 K/4.0/–3.0).
- For the giants we used two models (4488 K/2.0/–3.0 and 5020 K/2.5/–3.0) from the CIFIST grid. They have both a gravity slightly higher than the ones in our sample of giants, but no closer 3D model is available at the moment.

From these computations we found that for [Fe/H] = –3, [Ca/H] = –2.6, the 3D correction for the subordinate lines of Ca I in turnoff and in giant stars is very small.

In giants, the 3D correction seems to be negligible also for the resonance line. But with the model of turnoff stars, we found for the resonance line a 3D correction of –0.44 dex, and therefore the 3D correction increases the discrepancy between the subordinate lines and the 422.67 resonance line.

To date, it is not well understood why the abundance of calcium deduced from the resonance line of Ca I is, at very low metallicity, lower than the abundance deduced from the subordinate lines. It would be interesting to repeat the 3D computations with more metal-poor models (not available today). A fully consistent 3D NLTE model atmosphere and line formation scheme is currently beyond our reach.

5. Results and discussion

In this section we adopt the Ca abundance deduced from the subordinate lines of Ca I (Table 1, Cols. 11 and 12).

In Fig. 7 we present the new relation between [Ca/Fe] and [Fe/H]. The error bar plotted in for the subordinate lines the figure is the quadratic sum of the error due to the uncertainty of the model and the random error of the Ca abundance derived from the subordinate lines. The agreement between the turnoff and the giant stars is excellent, the ratio [Ca/Fe] is constant in the interval $-4.5 <$ [Fe/H] < -2.5. The slope of the regression line is –0.05. The scatter of [Ca/Fe] is a little smaller when NLTE effects are taken into account: 0.09 from NLTE computations compared to 0.10 from LTE computation.

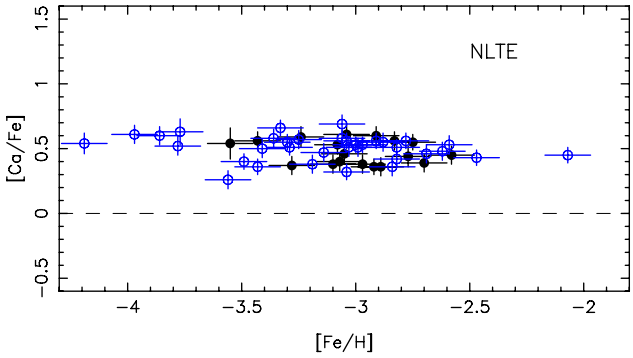

Fig. 7. [Ca/Fe] vs. [Fe/H] in our sample of EMP stars. Symbols as in Fig. 5. Turnoff and giant stars agrees quite well, [Ca/Fe] is constant in the range $-4.3 <$ [Fe/H] < -2.5 and the mean value is equal to [Ca/Fe] = 0.5, a value slightly higher than the LTE value [Ca/Fe] = 0.35 (see Bonifacio et al. 2009).

Table 3. Mean value of the ratios [X/Fe], [X/Ca] and [X/Mg] in the interval $-3.6 <$ [Fe/H] < -2.5 and scatter around the mean.

X	$\overline{\rm [X/Fe]}$	$\sigma_{\rm Fe}$	$\overline{\rm [X/Mg]}$	$\sigma_{\rm Mg}$	$\overline{\rm [X/Ca]}$	$\sigma_{\rm Ca}$
O	0.67	0.17	0.07	0.20	0.23	0.22
Na	–0.22	0.11	–0.82	0.14	–0.70	0.11
Mg	0.68	0.13	–	–	0.12	0.11
Al	–0.10	0.11	–0.71	0.11	–0.58	0.13
S	0.31	0.12	–0.31	0.15	–0.19	0.12
K	0.31	0.09	–0.32	0.15	–0.18	0.10
Ca	0.49	0.10	–0.12	0.11	–	–

In Fig. 8 we present the behavior of the abundances of O, Na, Mg, Al, S and K relative to Ca. The computation of these abundances take into account the NLTE effects (Andrievsky et al. 2007, 2008, 2010; and Spite et al. 2011). Since the abundance of oxygen has been determined from the forbidden oxygen line at 630 nm (Cayrel et al. 2004), it is free of NLTE effects.

In Fig. 8, different symbols are used for mixed and unmixed giants. After Spite et al. (2005, 2006) we call "mixed giants", those where, owing to mixing with deep layers, carbon has been partially transformed into nitrogen ([C/N] < -0.6), part of ^{12}C has been transformed into ^{13}C (^{12}C/^{13}C < 10), and lithium is not detected (lithium has been severely depleted by this mixing). In the HR diagram, these "mixed giants" are located above the "bump". It has been found (Andrievsky et al., 2007) that some mixed giants are enriched in sodium, this is visible in Fig. 8b. This Na-enhancement reflects a deep internal mixing (or an AGB status, or a contamination by AGB stars), but it does not reflect an anomaly of the chemical composition of the cloud that formed the star. Therefore the mixed stars cannot be used to determine the ratio [Na/Ca] in the early galactic matter.

Since the abundance ratios of O, Na, Al, S, and K relative to Ca are fairly flat vs. [Fe/H] in the central part of the diagram, we can define a mean value in this central interval, say $-3.6 <$ [Fe/H] < -2.5 as has been done with Mg in Andrievsky et al. (2010). The mean values of [X/Fe], [X/Mg] and [X/Ca] are given in Table 3 with the corresponding scatter. However, an

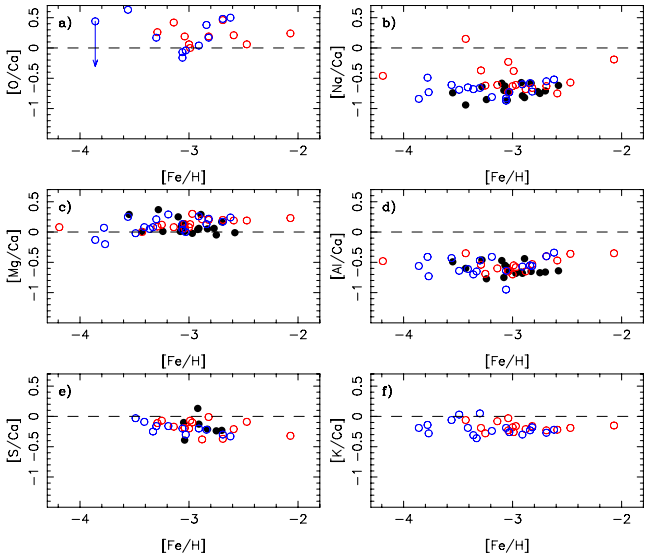

Fig. 8. Abundance ratios of O, Na, Mg, Al, S, and K relative to Ca in the early Galaxy. The abundances of all these elements were computed taking into account the NLTE effect. The black dots represent the turnoff stars, the open circles the giants (blue for the unmixed giants and red for the mixed giants).

anti-correlation seems to exist between [S/Ca] and [Fe/H] and also [S/Mg] and [Fe/H]: the Kendall τ coefficient is 98.9% for [S/Ca] and 99.1% for [S/Mg]. In these computations the weight of BD +17°3248 ([Fe/H] = –2.2) is important. This star is quite peculiar: according to For & Sneden (2010) it is a red horizontal branch star strongly enriched in heavy elements (Cowan et al. 2002). However, if this star is removed from the computations, the Kendall τ coefficient remains high: 97.6% for [S/Ca] and 97.9% for [S/Mg].

One turnoff star, BS 16023-046, and one unmixed giant CS 22956-50, have abnormally strong and broad sodium D lines. Their radial velocity (–7.5 km s^{-1} and –0.1 km s^{-1}) is low, and the stellar lines are very probably blended with interstellar lines. These stars have not been plotted on Fig. 8b and were not taken into account in computing the mean value and the scatter of [Na/Fe], [Na/Mg] and [Na/Ca] in Table 3.

It is interesting to take advantage of the high quality of the data to compare in Table 3 the scatter around the mean value when Fe, Mg, or Ca are taken as reference elements. The scatter of [O/Fe], [O/Mg] or [O/Ca] is fairly large: about 0.2 dex but this can be explained by the scatter of the oxygen abundance due to the reduced number of oxygen lines and the difficulty of the measurements. For the other ratios the scatter lies between 0.09 and 0.15 dex and we consider that this difference of 0.06 dex is significant. The scatter is always significantly smaller when Ca is taken as the reference element, with two exceptions:

- Oxygen: but in this case we have seen that the scatter is dominated by the error on the measurement of the very weak oxygen line.
- Aluminum: Al is better correlated with Mg than with Ca. But this correlation (opposite to the well known anti-correlation found in globular cluster stars) has at least one exception: CS 29516-024 is rather Al-poor but it is (relatively) Ca-rich and Mg-rich, and it does not seem possible to explain these differences by errors of measurements. A similar correlation between [Al/Fe] and [Mg/Fe] has been also suggested by Suda et al. (2011) even in a large but very inhomogeneous sample of metal-poor stars.

6. Concluding remarks

We determined the calcium abundance in a homogeneous sample of of 53 metal-poor stars (31 of them with [Fe/H] < –2.9) taking into account departures from LTE. We have shown that the trend of the ratio [Ca/Fe] vs. [Fe/H], below [Fe/H] = –2.7 is almost flat and derived a new mean value of [Ca/Fe] in the early Galaxy: [Ca/Fe] = 0.5 ± 0.09.

Generally speaking, our NLTE calculations agree quite well with those of Mashonkina et al. (2007). However, Mashonkina et al. had found different Ca abundances from the Ca I and Ca II lines in Procyon. With our new model atom of calcium, we are able to reconcile the calcium abundance deduced from neutral and ionized calcium lines in Procyon. We derived $\log \epsilon$(Ca) = 6.25 ± 0.04 from Ca I lines and 6.27 ± 0.06 from Ca II lines (6.33 and 6.40 under the LTE hypothesis). Moreover, the calcium abundance is found to be solar, as expected.

In metal-poor stars (below [Ca/H] = –2.5), a discrepancy clearly appears between the Ca abundances deduced from either the resonance Ca I line, or the Ca I subordinate lines. A rough estimation of the effect of convection on the profile of these lines does not explain this discrepancy.

In the stars of our sample (giants and turnoff stars) the wavelengths of the calcium lines are shifted by convection as a function of the equivalent width of the lines as has been found for the iron lines by Ramírez et al. (2010) in HD 122563.

The scatter around the mean value of [Ca/Fe] is small but since the NLTE correction is about the same for all the subordinate lines used in this analysis, the scatter is almost the same as it was in the LTE analyses (Cayrel et al. 2004; Bonifacio et al. 2009).

The abundance of the light metals O, Na, Al, S, K is well correlated with the calcium abundance. The correlation is generally a little better than it is with the magnesium abundance (with exception of the tight aluminium/magnesium correlation). However, it is striking that in Table 3, even when NLTE is taken into account, the correlation of the light elements O, Na, Al, S, K with Ca or Mg (all supposed to be formed mainly by hydrostatic fusion of C, Ne or O), is never better than the correlation with iron, providing some support to supernovae models predicting nucleosynthesis of all these elements predominantly in explosive modes (e.g. Nomoto et al. 2006).

Acknowledgements. The authors thank the referee, who indicated new $\log gf$ values for the high excitation Ca II lines. This work has been supported in part by the "Programme National de Physique Stellaire" (CNRS). S.A. kindly thanks the Observatoire de Paris, the CNRS, and the laboratory GEPI for their hospitality and support during his stay in Meudon. He acknowledges the National Academy of Sciences of Ukraine and the franco-Ukrainian exchange program for its financial support under contract UKR CDIV N24008.

References

Allen, C. W. 1973, Astrophys. Quant. (London: Athlone Press)
Alonso, A., Arribas, S., & Martínez-Roger, C. 1996, A&A, 313, 873
Alonso, A., Arribas, S., & Martínez-Roger, C. 1999, A&AS, 140, 261
Alonso, A., Arribas, S., & Martínez-Roger, C. 2001, A&AS, 376, 1039
Andrievsky, S., Spite, M., Korotin, S., et al. 2007, A&A, 464, 1081
Andrievsky, S. M., Spite, M., Korotin, S. A., et al. 2008, A&A, 481, 481
Andrievsky, S., Spite, M., Korotin, S., et al. 2010, A&A, 509, A88
Anstee, S. D., & O'Mara, B. J. 1995, MNRAS, 276, 859
Asplund, M., Grevesse, N., Sauval, J., & Scott, P. 2009, ARA&A, 47, 481
Bagnulo, S., Jehin, E., Ledoux, C., et al. 2003, The Messenger, 114, 10
Barklem, P. S., & O'Mara, B. J. 1997, MNRAS, 290, 102
Barklem, P. S., & O'Mara, B. J. 1998, MNRAS, 300, 863
Barklem, P. S., O'Mara, B. J., & Ross, J. E. 1998, MNRAS, 296, 1057
Bonifacio, P., Molaro, P., Sivarani, T., et al. 2007, A&A, 462, 851
Bonifacio, P., Spite, M., Cayrel, R., et al. 2009, A&A, 501, 519

Burgess, A., Chidichimo, M. C., & Tully, J. A. 1995, A&A, 300, 627
Caffau, E., & Ludwig, H.-G. 2007, A&A, 467, L11
Carlsson, M. 1986, Uppsala Obs. Rep., 33
Cayrel, R., Depagne, E., Spite, M., et al. 2004, A&A, 416, 1117
Cowan, J. J., Sneden, C., Burles, S., et al. 2002, ApJ, 572, 861
Dekker, H., D'Odorico, S., Kaufer, A., Delabre, B., & Kotzlowski, H. 2000, Proc. SPIE, 4008, 534
For, B.-Q., & Sneden, C. 2010, AJ, 140, 1694
Freytag, B., Steffen, M., & Dorch, B. 2002, AN, 323, 213
Freytag, B., Steffen, M., Ludwig, H.-G., et al. 2011, JCoPh, 231, 919
González Hernández, J. I., Bonifacio, P., Ludwig, H.-G., et al. 2010, A&A, 519, A46
Grevesse, N., & Sauval, A. J. 2000, Origin of the elements in the solar system, Implications of post-1957 Observations, ed. O. Manuel (Kluwer Academic/Plenum Publishers), 261
Hirata, R., & Horaguchi, T. 1995, Catalogue of Atomic Spectroscopic Lines (Strasbourg: CDS), 6, 69
Hosford, A., Ryan, S. G., Garcia Perez, A. E., Norris, J. E., & Olive, K. A. 2009, A&A, 493, 601
Ivanova, D. V., Sakhibullin, N. A., & Shimanskii, V. V. 2002, ARep, 46, 390
Kobayashi, Ch., Umeda, H., Nomoto, K., et al. 2006, ApJ, 653, 1145
Korn, A., Shi, J., & Gehren, T. 2003, A&A, 407, 691
Korotin, S. A. 2008, Odessa Astronomical Pub., 21, 42
Korotin, S. A., Andrievsky, S. M., & Luck, R. E. 1999, A&A, 351, 168
Kurucz, R. L. 1992, RMxAA, 23, 181
Kurucz, R. L. 1993, SAO, Cambridge, CDROM18
Kurucz, R. L., & Bell, B. 1995, SAO, Cambridge, CDROM23
Kurucz, R. L., Furenlid, I., Brault, J., & Testerman, L. 1984, National Solar Observatory Atlas, Sunspot, New Mexico: National Solar Observatory
Lodders, K., Plame, H., & Gail, H.-P. 2009, in Landolt-Börnstein, New Series, Vol. VI/4B, Chap. 4.4, ed. J. E. Trümper (Berlin Heifelberg New York: Springer-Verlag), 560
Ludwig, H.-G., Behara, N. T., Steffen, M., & Bonifacio, P. 2009, A&A, 502, L1
Magain, P. 1988, in The impact of Very High S/N spectroscopy on Stellar Physics, ed. G. Cayrel de Strobel, & M. Spite (Dordrecht, Kluwer), IAU Symp., 132, 485
Mashonkina, L., Gehren, T., Travaglio, C., & Borkova, T. 2003, A&A, 397, 275
Mashonkina, L., Korn, A. J., & Przybilla, N. 2007, A&A, 461, 261
Meléndez, M., Bautista, M. A., & Badnell, N. R. 2007, A&A, 469, 1203
Merle, T., Thévenin, F., Pichon, B., & Bigot, L. 2011, MNRAS, 418, 863
Morton, D. C. 1991, ApJS, 77,119
Nomoto, K., Tominaga, N., Umeda, H., et al. 2006, Nucl. Phys. A, 777, 424
Perryman, M. A. C., Lindegren, L., Kovalevsky, J., et al. 1997, A&A, 323, L49
Ramírez, I., Collet, R., Lambert, D. L., Allende Prieto, C., & Asplund, M. 2010, ApJ, 725, L223
Rutten, R. J., Hammerschlag, R. H., Bettonvil, F. C. M., Sütterlin, P., & de Wijn, A. G., 2004, A&A, 413, 1183
Ryan, S. G., Norris, J. E., & Beers, T. C. 1996, ApJ, 471, 1996
Samson, A. M., & Berrington, K. A. 2001, ADNDT, 77, 87
Seaton, M. J. 1962, in Atomic and Molecular processes (New York: Academic Press)
Smith, G. 1988, J. Phys. B, 21, 2827
Smith, G., & Raggett, D. St. J. 1981, J. Phys. B, 14, 4015
Spite, M., Cayrel, R., Plez, B., et al. 2005, A&A, 430, 655
Spite, M., Cayrel, R., Hill, V., et al. 2006, A&A, 455, 291
Spite, M., Caffau, E., Andrievsky, S., et al. 2011, A&A, 528, A9
Steenbock, W., & Holweger, H. 1984, A&A, 130, 319
Suda, T., Yamada, S., Katsuta, Y., et al. 2011, MNRAS, 412, 843
Sugar, J., & Corliss, C. 1985, J. Phys. Chem. Ref. Data, 14
Theodosiou, C. E. 1989, Phys. Rev. A, 39, 4880
Van Regemorter, H. 1962, ApJ, 136, 906
Vernazza, J. E., Avrett, E. H., & Loeser, R. 1981, ApJS, 45, 635
Wiese, W. L., & Martin, G. A. 1980, NSRDS-NBS 68, Part II
Wiese, W. L., Smith, M. W., & Miles, B. M. 1969, NSRDS-NBS, 22, 2